Heterogeneously integrated III-V on silicon multi-bandgap superluminescent light emitting diode with 290nm optical bandwidth

A. De Groote,[1,2,*] J.D. Peters,[1] M.L. Davenport,[1] M.J.R. Heck,[1] R. Baets,[2] G. Roelkens,[2] and J.E. Bowers[1]

[1] *Optoelectronics Research Group, ECE Dept., University of California Santa Barbara, United States*

[2] *Photonics Research Group, Dept. of Information Technology, Ghent University - imec, Belgium*

compiled: June 3, 2014

For the first time, quantum well intermixing and multiple die bonding of InP on a silicon photonic waveguide circuit were combined. In this manner, a broadband superluminescent III-V on silicon LED was realized. The device consists of four sections with different band gaps, centered around 1300nm, 1380nm, 1460nm and 1540nm. The fabricated LEDs were connected on-chip in a serial way, where the light generated in the smaller band gap sections travels through the larger band gap sections. By balancing the pump current in the four LEDs we achieved 292nm of 3dB bandwidth and an on-chip power of -8dBm.

OCIS codes: (130.3120) Integrated optics devices; (230.3670) Light-emitting diodes; (230.5590) Quantum-well, -wire and -dot devices; Silicon Photonics

http://dx.doi.org/10.1364/XX.99.099999

While originally conceived for data and telecom applications, a broader range of applications is rapidly emerging using silicon photonics as a potential integration platform. Using standard CMOS fabrication techniques the silicon photonic chip fabrication can achieve very high yield. However, it is difficult to realize a monolithically integrated light source on silicon due to its indirect band gap. Therefore III-V compounds such as InP are heterogeneously integrated on silicon-on-insulator (SOI) waveguide circuits. In these integrated devices the gain is provided by the active region originally grown on a III-V substrate. [1] [2] [3]

Superluminescent diodes (SLDs) are suitable for numerous applications ranging from optical component testing to sensing applications (e.g. gyroscopes) as well as medical imaging (e.g. optical coherence tomography). For these applications, large bandwidth is of critical importance (300nm of bandwidth leads to $\pm 3\mu$m of resolution in OCT). There are different approaches of extending the bandwidth of the III-V gain medium, among which a dual quantum well design [4], multistate quantum wells [5] and quantum dots [6]. These structures are however difficult to design and optimize and operate well only using specific drive currents. Alternatively, broadband supercontinuum sources can be considered, but these typically require ultra-short pulse sources that cannot yet be integrated on the silicon-on-insulator waveguide circuit [7].

To address these limitations, we designed and demonstrated a superluminescent single mode light emitting diode with different active sections having a different band gap, integrated on a silicon waveguide circuit. Thanks to the implantation enhanced disordering quantum well intermixing technique (IED-QWI), we can blueshift certain areas of the to-be-bonded InP die [8]. On top of that, we can bond several dies on one SOI waveguide circuit [9]. To our knowledge, it is the first time that these two techniques have been combined, although they are very complementary. With this achievement, we merged four different band gaps in a serial manner, as indicated in figure 1a.

Since two epitaxial layer stacks are bonded side by side, we have a large design freedom for the epitaxial design. Our layer stack of choice is described in table 1. The downside of this multiple die bonding is the reduced flexibility in the positioning of the different materials. If one would only use this technique, four different dies have to be bonded next to each other. Consequently the device area grows very large. Quantum well intermixing is a technique of changing the composition of the quantum wells by atom disordering. As this is lithographically defined, it does give us this extra flexibility and makes it possible to have two band gaps in the same mesa. The maximum wavelength shift is limited

* Corresponding author: andreasdegroote@intec.ugent.be

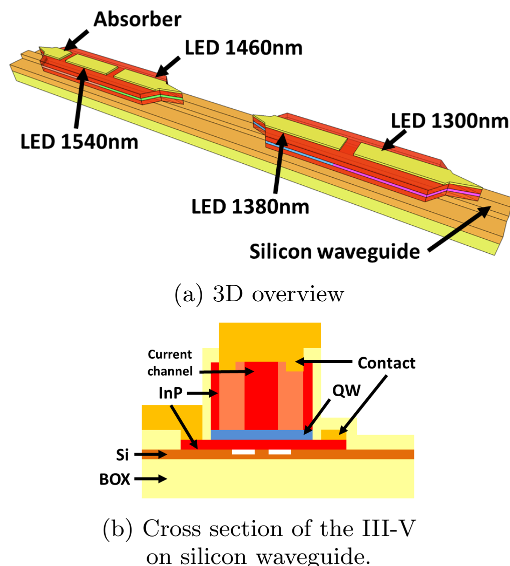

(a) 3D overview

(b) Cross section of the III-V on silicon waveguide.

Fig. 1: Illustration of the broadband LED

to ±125nm around telecom wavelengths though, as discussed in the next section.

Because of this, our structures were designed such that each device has two mesas, each consisting of two band gaps, as indicated in figure 1. The narrowest band gap is utmost left, the largest is utmost right. This way the light can travel towards the right without suffering from strong band-to-band absorption. Any photons traveling towards the left are absorbed by the narrower band gaps, thereby optically pumping the narrow band gap material. In this manner, we have created a one-directional device which only emits on the right side. In the design of an LED, special precautions have to be taken to prevent lasing, which would narrow the spectrum. Here, inherently it is impossible to lase for all band gaps because the band gap to the left will always heavily absorb the generated light, so no net roundtrip gain is possible. This is true for all band gaps except the smallest one. Therefore, we created an extra absorbing section on the left side, by reverse biasing part of the active waveguide.

Fabrication starts with the preparation of two InP samples. The epitaxial layer stack is depicted in table 1. First alignment markers are etched, in order to be able to do an aligned bonding. To avoid delamination during bonding they have to be lower than the bonding surface, layer 7 in table 1, so they are etched in two steps (first a wide window in layers #8 and #9, then the actual marker in layer #6 and #7). The to-be-intermixed areas are implanted with phosphor ions into the buffer layer (#9). Subsequently, they are propagated into the quantum wells during a 700°C/725°C thermal anneal. Because phosphor starts to evaporate at 500°C at atmospheric pressure [10], a cap layer is necessary (a SiN/SiO2/SiN strain compensated layer). Figure 2 shows the evolution of the PL peak wavelengths (both in absolute terms and relative to each other) as a function of time for the two materials. In figure 2b, one can clearly see that the maximum shift is 125nm. At longer anneal duration, the implanted areas cease to intermix, probably because the atom gradient is not high enough any more. The QW becomes shallow and the location of the eigenstates are hard to shift. The non-implanted areas on the other hand start to shift: the thermal energy is high enough to start atom disordering without the addition of impurities. An alternative explanation would be that the growth defects start to act as initiator of disordering. After quantum well intermixing the buffer layer is etched away, leaving a clean, flat bonding surface (#7). The PL spectra of the different materials are shown in figure 3, illustrating a broad wavelength coverage.

In the SOI sample, trenches of 250nm deep are dry etched in the 500nm thick silicon device layer to form the waveguide, followed by the etching of vertical outgassing channels, which increase the bonding yield. Plasma-assisted bonding is carried out as described in [11]. Note that in this work, the SOI and InP dies have to be aligned during bonding. Using a flip chip bonder both dies were placed consecutively, with an alignment error of 2μm. After die attachment, both dies are annealed at the same time, creating the strong covalent bonds. Because the post bond process contains a few dry etches which might damage the silicon waveguides in between the dies, 1μm thick low-temperature PECVD SiO_2 was deposited. This forms a thick barrier both for the damage of dry etches as well as for preventing wet etchants to enter the waveguide trenches. After this, the InP substrates of both dies are removed, with a combination of mechanical polishing and wet etching. Because of the mechanical removal, the deposited oxide is milled away, opening the InP dies in a self-aligned manner.

The post bond process starts with mesa definition. RIE etching was used to etch down into the QW layer, and then a selective wet etch stopped on the n-InP layer. Pd/Ti/Pd/Au and Pd/Ge/Pd/Au were deposited

#	Layer	Thickness	Doping
9	Sacrificial InP buffer	450 nm	i
8	$In_{0.8423}GaAs_{0.3434}P$ etch stop	40 nm	i
7	n-InP bonding layer	17.5 nm	(n) $3 \times 10^{18}cm^{-}3$
6	$In_{0.85}GaAs_{0.327}P$/InP superlattice	(2x) 7.5/7.5 nm	(n) $3 \times 10^{18}cm^{-}3$
5	n-InP contact	110 nm	(n) $3 \times 10^{18}cm^{-}3$
4a	$In_{0.741}GaAs_{0.805}P$ well / $In_{0.9611}GaAs_{0.0025}P$ barrier	7x4.0 / 8x8.0 nm	i
4b	$In_{0.735}GaAs_{0.845}P$ well / $In_{0.735}GaAs_{0.513}P$ barrier	7x6.5 / 8x8.0 nm	i
3	p-$In_{0.5305}Al_{0.4055}Ga_{0.064}As$	250 nm	(p) $10^{17}cm^{-}3$
2	p-InP	1.5 μm	(p) $10^{18}cm^{-}3$
1	p-$In_{0.532}GaAs$	100 nm	(p) $10^{19}cm^{-}3$
0	p-InP substrate	350 μm	(p) $2 \times 10^{18}cm^{-}3$

Table 1: Epitaxial layer stack. The stack with layers 4a as QWs has a PL peak at 1380nm, the one with layers 4b has a PL peak at 1540nm.

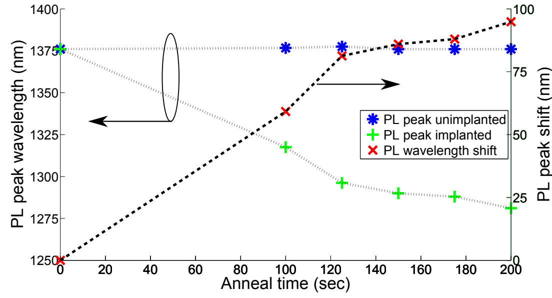

(a) Epitaxial layer stack designed for 1380nm. Anneal temperature 700°C.

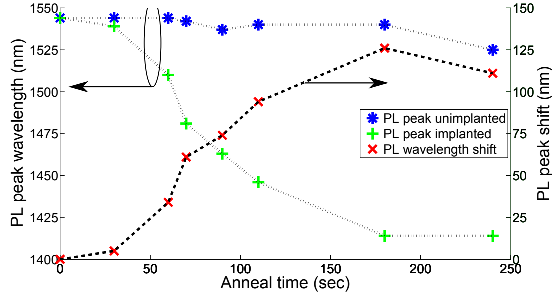

(b) Epitaxial layer stack designed for 1540nm.Anneal temperature 725°C.

Fig. 2: Evolution of photoluminescence peak wavelength as a function of time of the different epitaxial layer stacks.

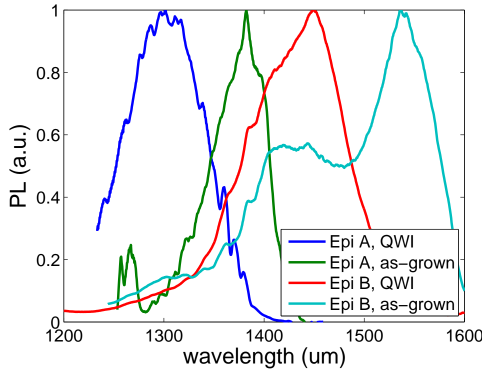

Fig. 3: Normalized photoluminescence data of two as-grown bands and shifted band gaps. The two epitaxial layer stacks are identical except for the quantum wells. Those of Epi A are designed for 1380nm, those of Epi B for 1540nm.

as contact metals for the p- and n-contacts respectively. The contact resistivity of these contacts was measured with the transmission line method (TLM) to be $3 \times 10^{-5} \Omega$ cm^2 for the p-contact, and $4 \times 10^{-7} \Omega$ cm^2 for the n-contact. The mesa was 24μm wide, so proton implantation was necessary to form a 4μm wide current channel. Finally, the different sections are isolated from each other, by etching the p-contact layer (InGaAs) and part of the p-InP. This rendered an electrical isolation of more than 50kΩ. Note that both bonded dies are processed at the same time. [12]

The tapers used to efficiently couple light from the III-V on silicon hybrid structure to the passive silicon waveguide are 20μm long and are 2-staged, with a narrow p-InP layer and a gradual taper in the quantum wells. The length of each band gap section is 1mm.

Figure 4 shows the CW performance of the fabricated device at 20C. Each section can be controlled separately, with the different P-contacts being isolated by more than 50kΩ. From the individual test structures on the chip, we know the output power of each section separately is very similar. Hence, from figure 4a we conclude that

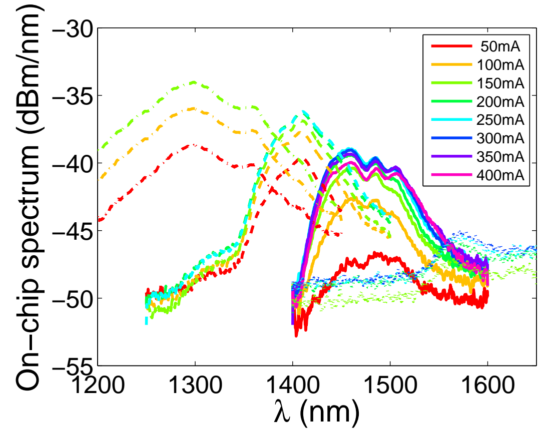

(a) Different sections pumped separately. We used a dashed, dash-dotted, full and dotted line for the section at 1300nm, 1380nm, 1460nm and 1540nm respectively.

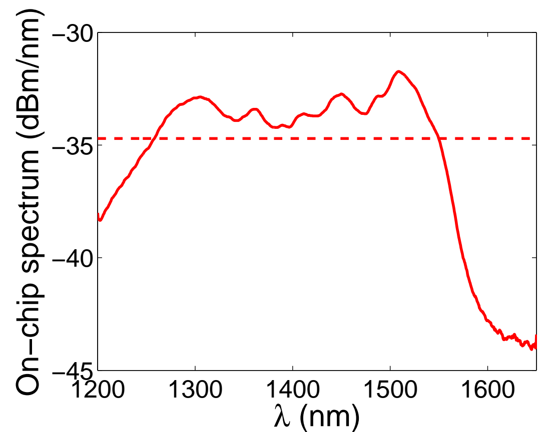

(b) Balanced pumping to optimize the 3dB band width. The pumping currents were 70mA, 50mA, 300mA and 140mA for the sections at 1300nm, 1380nm, 1460nm and 1540nm respectively.

Fig. 4: On-chip spectra of the depicted device.

there is considerable loss in the system. The longest wavelengths have to travel furthest through the structures, and their power is lowest.

The different currents are chosen such that we have a broad, flat-top spectrum as shown in figure 4b. The pump current was 70mA, 50mA, 300mA and 140mA for the sections at 1300nm, 1380nm, 1460nm and 1540nm respectively. A total on-chip power of -8dBm is achieved with a 3dB bandwidth of 292nm. The O,E,S and part of the C band were covered, ranging from 1258nm to 1550nm.

It can be concluded that the loss, which was observed in figure 4a, is mainly due to residual absorption in the quantum wells the light has to travel through. When all sections are pumped, the difference in power is nearly gone.

From the dotted line in figure 4a, one may conclude that that section emits at 1580nm rather than 1540nm. This is contradicted by our measurement of the backside emission of the absorbing section (when forward biasing it), which does show a maximum at 1540nm (not shown here). Also here the residual absorption is to blame. Since this absorption is below-band-gap-absorption, it is highly dependent on the wavelength. The shorter wavelengths are much more absorbed than the longer ones. Light is generated with a maximum around 1540nm, but the shorter wavelengths are absorbed. Since we measure the product of both emission and absorption the measured maximum is 1580nm rather than 1540nm. A similar behaviour is seen in figure 4b, where the maximum at 1500nm is highly dependent on the pumping conditions of both sections. Instead of absorption, there is below band gap gain. This highly asymmetric gain profile amplifies the shorter wavelengths much more than the longer, causing the maximum to shift to 1500nm rather than 1540nm.

For the first time, quantum well intermixing and multiple die bonding were combined. In this manner, we have realized a broadband, single mode LED coupled to a silicon waveguide. Four different band gaps were created and merged in order to cover the O,E,S and C band. The device was designed to be one-directional by arranging the band gaps from narrow to wide. When pumping the different sections to achieve a flat top spectrum, we managed to achieve 292nm 3dB bandwidth, while the total power was -8dBm.

This research was supported by DARPA MTO under the EPHI contract and the FP7-ERC-InSpectra project. Andreas De Groote thanks the research foundation Flanders (FWO) for a research grant and also the Belgian American Educational Foundation (BAEF) for the support.

References

[1] S. Keyvaninia, S. Verstuyft, L. Van Landschoot, D. Van Thourhout, G. Roelkens, G. Duan, , F. Lelarge, J. Fedeli, S. Messaoudene, T. De Vries, B. Smalbrugge, E. Geluk, J. Bolk, and M. Smit, "Heterogeneously integrated iii-v/silicon distributed feedback lasers," *Optics letters*, vol. 38, no. 24, pp. 5434–5437, 2013.

[2] M. Heck, J. F. Bauters, M. L. Davenport, J. K. Doylend, S. Jain, G. Kurczveil, S. Srinivasan, Y. Tang, and J. E. Bowers, "Hybrid silicon photonic integrated circuit technology," *IEEE Journal of Selected Topics in Quantum Electronics*, vol. 19, no. 4, 2013.

[3] G. Roelkens, L. Liu, D. Liang, R. Jones, A. Fang, B. Koch, and J. Bowers, "III-V/silicon photonics for on-chip and intra-chip optical interconnects," *Laser & Photonics Reviews*, vol. 4, no. 6, pp. 751–779, 2010.

[4] B.-R. Wu, C.-F. Lin, L.-W. Laih, and T.-T. Shih, "Extremely broadband ingaasp/inp superluminescent diodes," *Electronics Letters*, vol. 36, no. 25, pp. 2093–2095, 2000.

[5] J. Song, S. Cho, I. Han, Y. Hu, P. Heim, F. Johnson, D. Stone, and M. Dagenais, "High-power broad-band superluminescent diode with low spectral modulation at 1.5-/spl mu/m wavelength," *Photonics Technology Letters, IEEE*, vol. 12, no. 7, pp. 783–785, 2000.

[6] A. Kovsh, A. Gubenko, I. Krestnikov, D. Livshits, S. Mikhrin, J. Weimert, L. West, G. Wojcik, D. Yin, C. Bornholdt, N. Grote, M. Maximov, and A. Zhukov, "Quantum dot comb-laser as efficient light source for silicon photonics," in *Photonics Europe*, pp. 69960V–69960V, International Society for Optics and Photonics, 2008.

[7] J. Safioui, F. Leo, B. Kuyken, S.-P. Gorza, S. K. Selvaraja, R. Baets, P. Emplit, G. Roelkens, and S. Massar, "Supercontinuum generation in hydrogenated amorphous silicon waveguides at telecommunication wavelengths," *Optics express*, vol. 22, no. 3, pp. 3089–3097, 2014.

[8] S. R. Jain, Y. Tang, H.-W. Chen, M. N. Sysak, and J. E. Bowers, "Integrated hybrid silicon transmitters," *Journal of Lightwave Technology*, vol. 30, no. 5, pp. 671–678, 2012.

[9] H.-H. Chang, A. W. Fang, M. N. Sysak, H. Park, R. Jones, O. Cohen, O. Raday, M. J. Paniccia, and J. E. Bowers, "1310nm silicon evanescent laser," *Optics Express*, vol. 15, no. 18, pp. 11466–11471, 2007.

[10] F. Riesz, L. Dobos, C. Vignali, and C. Pelosi, "Thermal decomposition of InP surfaces: volatile component loss, morphological changes, and pattern formation," *Materials Science and Engineering: B*, vol. 80, no. 1, pp. 54–59, 2001.

[11] D. Liang and J. Bowers, "Highly efficient vertical outgassing channels for low-temperature inp-to-silicon direct wafer bonding on the silicon-on-insulator substrate," *Journal of Vacuum Science & Technology B*, vol. 26, no. 4, pp. 1560–1568, 2008.

[12] C. Zhang, S. Srinivasan, Y. Tang, M. J. Heck, M. L. Davenport, and J. E. Bowers, "Low threshold and high speed short cavity distributed feedback hybrid silicon lasers," *Optics Express*, vol. 22, no. 9, pp. 10202–10209, 2014.